

Новые результаты коллабораций

CBELSA/TAPS (Бонн) и Crystal Ball at MAMI, TAPS and A2 (Майнц)

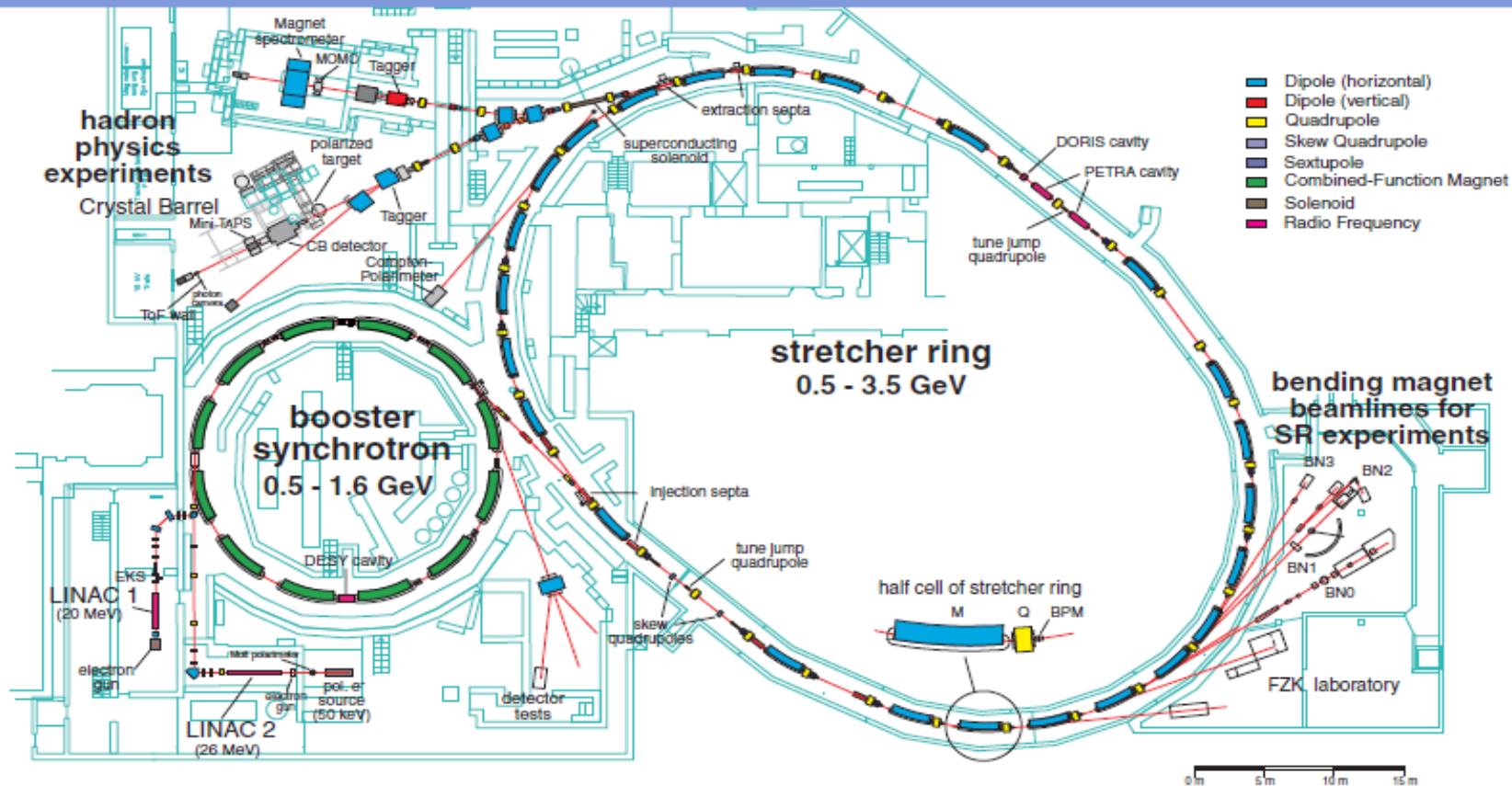
Гамма-нульон

Участники коллаборации **CBELSA/TAPS** (Бонн)
от Лаборатории мезонной физики:

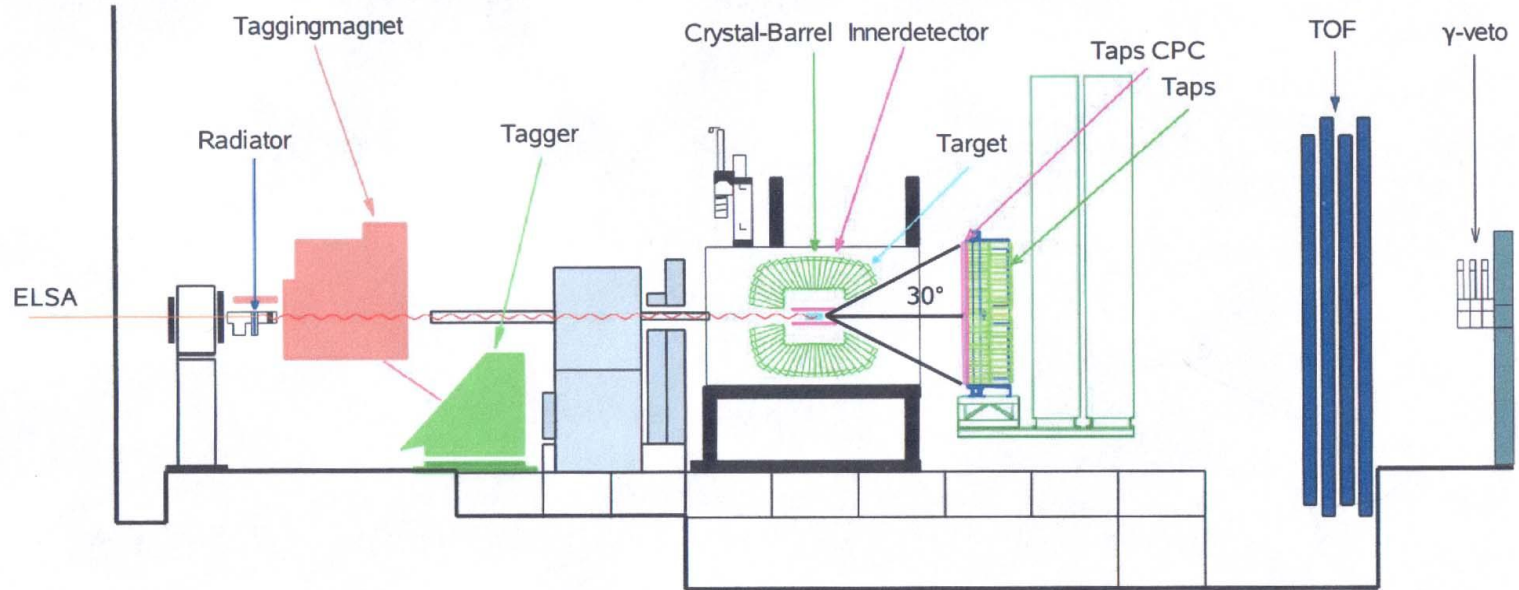
Д.Е. Баядилов, Ю.А. Белоглазов, А.Б. Гриднев, И.В. Лопатин,
Д.В. Новинский, А.К. Радьков, В.В. Сумачёв.

Ускоритель - ELectron Stretcher Anlage (ELSA)

- Energy range 0.5–3.5 GeV
- Max. extracted intensity $\sim 1\text{nA}$
- Electron polarisation $\sim 60\text{--}80\%$



Experimental Setup



3.3 GeV E_{electron}

up to 3 GeV photons

LH_2/LD_2 1290 CsI crystals

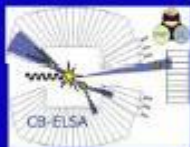
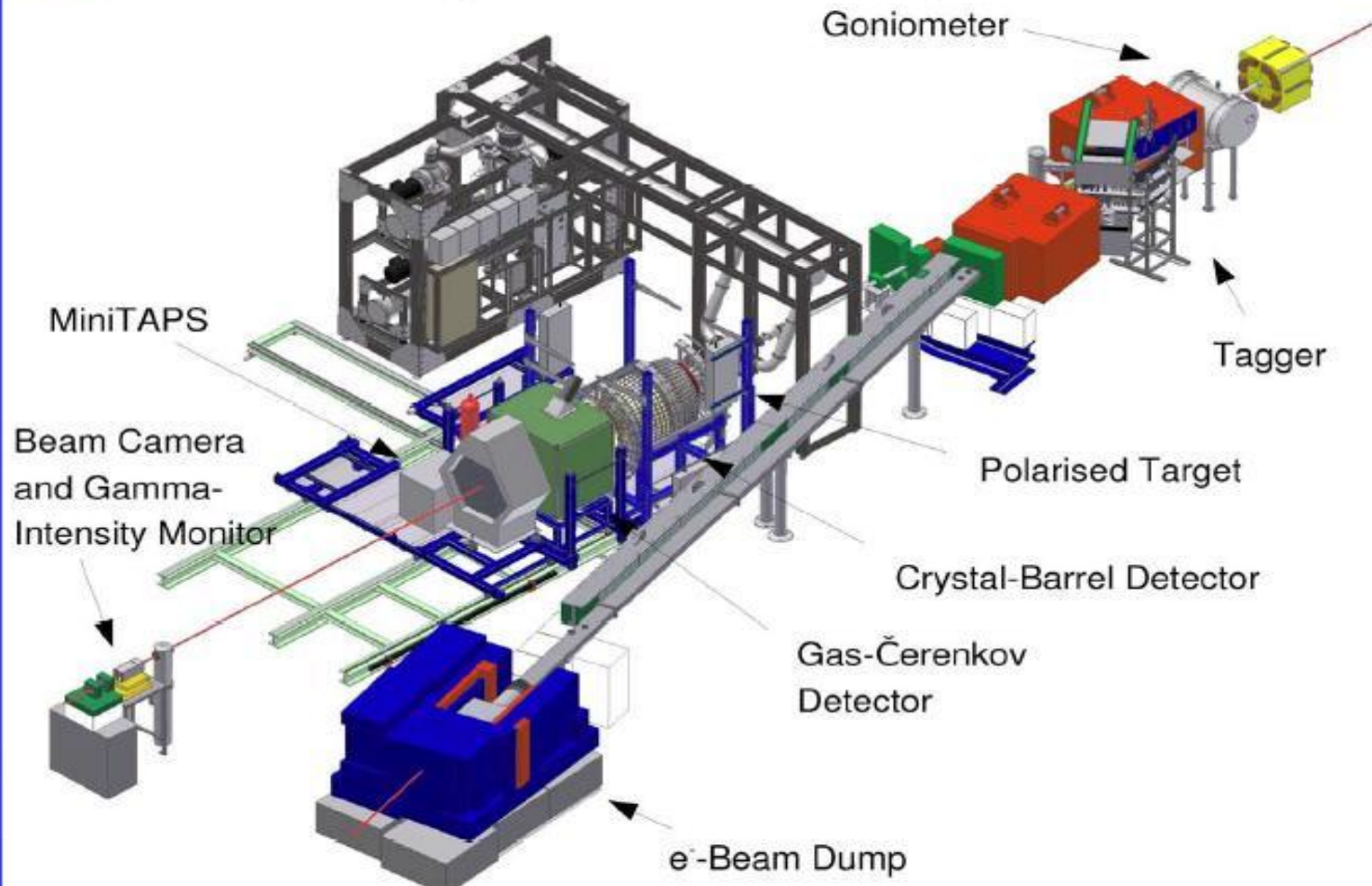
522 BaF crystals

4π geometry, high sensitivity to multiphoton final states
physics aims:
meson production and baryon spectroscopy

Схема установки CB-ELSA

universität**bonn**

The Crystal-Barrel Experiment



(GAMMA-NUCLEON)

Photon		Target	Recoil	Target-Recoil
		$x \quad y \quad z$	$x' \quad y' \quad z'$	$x' \quad x' \quad z' \quad z'$ $x \quad z \quad x \quad z$
unpolarized	σ	$0 \quad T \quad 0$	$0 \quad P \quad 0$	$T_{x'} \quad -L_{x'} \quad T_{z'} \quad L_{z'}$
linearly	$-\Sigma$	$H \quad (-P) \quad -G$	$O_{x'} \quad (-T) \quad O_{z'}$	$(-L_{z'}) \quad (T_{z'}) \quad (-L_{x'}) \quad (-T_{x'})$
circularly	0	$F \quad 0 \quad -E$	$C_{x'} \quad 0 \quad C_{z'}$	$0 \quad 0 \quad 0 \quad 0$

- the 4 independent helicity amplitudes of single pseudoscalar meson photoproduction can be uniquely determined by 8 out of 16 accessible observables, among:
 - 4 double polarization observables (at least 2 recoil observables),
 - 2 with transversally polarized target,
- with transversally polarized target, P can be measured without measuring the polarization of the recoil proton
- complete set: $\Sigma, \sigma, T, P, G, E, C_{x'}, C_z$
- $C_{x'}, C_z$ are measured for single π production (Phy. Rev. C66 034614 2002)
 - with these measurements a complete experiment is possible

Well-established nucleon resonances revisited by double-polarization measurements

A. Thiel,¹ A.V. Anisovich,^{1,2} D. Bayadilov,^{1,2} B. Bantes,³ R. Beck,¹ Yu. Beloglazov,^{1,2} M. Bichow,⁴ S. Böse,^{1,5} K.-Th. Brinkmann,^{1,5} Th. Challand,⁶ V. Crede,⁷ F. Dietz,⁵ P. Drexler,⁵ H. Dutz,³ H. Eberhardt,³ D. Elsner,³ R. Ewald,³ K. Fornet-Ponse,³ St. Friedrich,⁵ F. Frommberger,³ Ch. Funke,¹ M. Gottschall,¹ M. Grüner,¹ E. Gutz,¹ Ch. Hammann,¹ J. Hannappel,³ J. Hartmann,¹ W. Hillert,³ Ph. Hoffmeister,¹ Ch. Honisch,¹ I. Jaegle,⁶ I. Jürgensen,¹ D. Kaiser,¹ H. Kalinowsky,¹ F. Kalischewski,¹ S. Kammer,³ I. Keshelashvili,⁶ V. Kleber,³ F. Klein,³ E. Klempt,¹ B. Krusche,⁶ M. Lang,¹ I. Lopatin,² Y. Maghrbi,⁶ K. Makonyi,⁵ V. Metag,⁵ W. Meyer,⁴ J. Müller,¹ M. Nanova,⁵ V. Nikonov,^{1,2} R. Novotny,⁵ D. Piontek,¹ G. Reicherz,⁴ A. Sarantsev,^{1,2} Ch. Schmidt,¹ H. Schmieden,³ T. Seifen,¹ V. Sokhoyan,¹ V. Sumachev,² U. Thoma,¹ H. van Pee,¹ D. Walther,¹ Ch. Wendel,¹ U. Wiedner,⁴ A. Wilson,⁷ A. Winnebeck,¹ and Y. Wunderlich¹

(The CBELSA/TAPS Collaboration)

Well-established nucleon resonances revisited by double-polarization measurements.

The first measurement is reported of the double-polarization observable G in photoproduction of neutral pions off protons, covering the photon energy range from 620 to 1120 MeV and the full solid angle. G describes the correlation between the photon polarization plane and the scattering plane for protons polarized along the direction of the incoming photon. The observable is highly sensitive to contributions from baryon resonances. The new results are compared to the predictions from SAID, MAID, and BnGa partial wave analyses. In spite of the long-lasting efforts to understand $\gamma p \rightarrow p\pi^0$ as the simplest photoproduction reaction, surprisingly large differences between the new data and the latest predictions are observed which are traced to different contributions of the $N(1535)$ with spin-parity $J^P = 1/2^-$ and $N(1520)$ with $J^P = 3/2^-$. In the third resonance region, where $N(1680)$ with $J^P = 5/2^+$ production dominates, the new data are reasonably close to the predictions.

GAMMA-HUNT

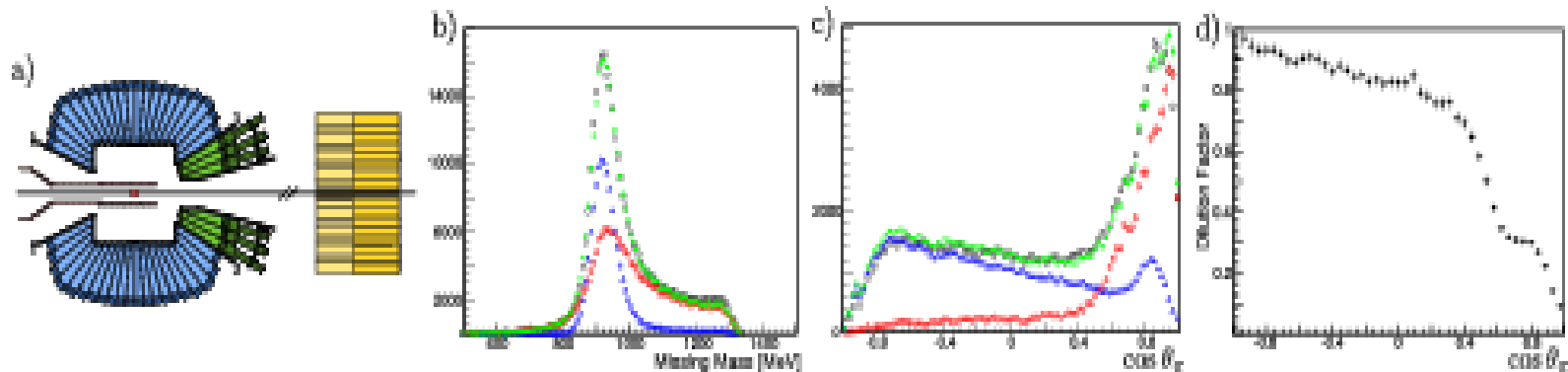


Figure 1. (Color online) a) The central part of the detector system. The CsI(Tl) crystals (blue and green) are read out via wavelength shifters and photodiodes or photomultipliers, BaF₂ crystals (yellow) in forward direction with photomultipliers. b) The missing mass distribution, and (c) the π^0 angular distribution for reaction (1) for an incident photon energy of $E_{\gamma} = 1000 \pm 25$ MeV; butanol (\square), hydrogen (\triangle), carbon (\diamond), and the sum of hydrogen and carbon data (\bullet). From these distributions, the dilution factor (d) is determined.

Linearly polarized photons were produced by scattering of a 3.3 GeV electron beam off a diamond crystal, whereby maximal polarization of 65% at 950 MeV and 59% at 1150 MeV for second data set were reached. The photons then hit a butanol (C₄H₁₀O) target with longitudinally polarized protons, with a mean proton polarization of about 75%. The butanol target was replaced by a hydrogen or carbon target for background studies and for normalization.

(GAMMA-HYDRON)

The incoming photons may produce a π^0 in the reaction



For linearly polarized photons (with polarization p_γ) and protons (with polarization p_T), the number of events N at the polar angle θ_π due to reaction (1) as a function of the azimuthal angle ϕ_π can be written in the form

$$\frac{N(\phi_\pi, \theta_\pi)}{N_0(\theta_\pi)} = 1 - p_\gamma \Sigma_B \cos(2\phi_\pi) + p_\gamma p_T G_B \sin(2\phi_\pi) \quad (2)$$

where N_0 is given by averaging $N(\phi_\pi, \theta_\pi)$ over ϕ_π . The beam asymmetry Σ_B and the observable G_B for the butanol target are related to the corresponding quantities for scattering off free (f) protons Σ, G and bound (b) nucleons by

$$\Sigma_B = \frac{N_0^f \Sigma + N_0^b \Sigma_b}{N_0^f + N_0^b}; \quad G_B = \frac{N_0^f}{N_0^f + N_0^b} \cdot G. \quad (3)$$

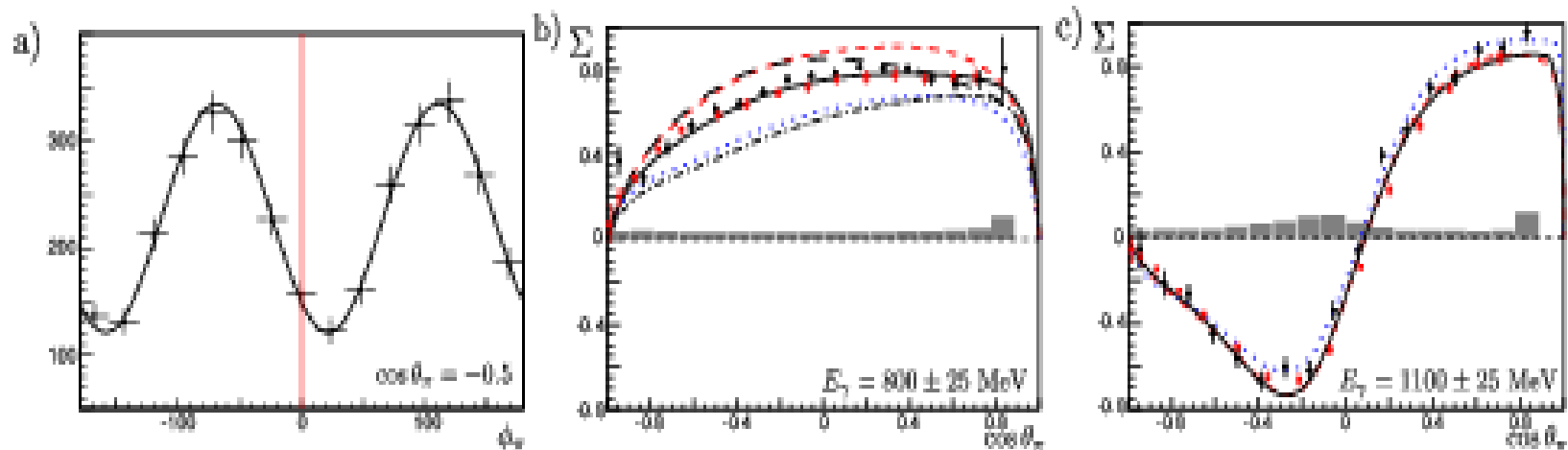


Figure 2. (Color online) a) A typical ϕ_γ -distribution with a fit using eq. (2). b,c) The beam asymmetry Σ as a function of $\cos \theta_\gamma$ for $E_\gamma = 800$ MeV and for $E_\gamma = 1100$ MeV. Black dots show our data, red squares GRAAL data [20]. The curves represent predictions from different partial wave analyses. Solid (black) curve: BnGa [24]; dashed (red): SAID [22]; long-dashed (black): BnGa with E_{0+} and E_{2-} amplitudes from SAID; dotted (blue): MAID [23]; dashed-dotted (black): BnGa with E_{0+} and E_{2-} amplitudes from MAID. Gray area shows the systematic error due to interactions on nuclei and uncertainty in the photon polarization.

ГAMMA-ИЗЛУЧЕНИЕ

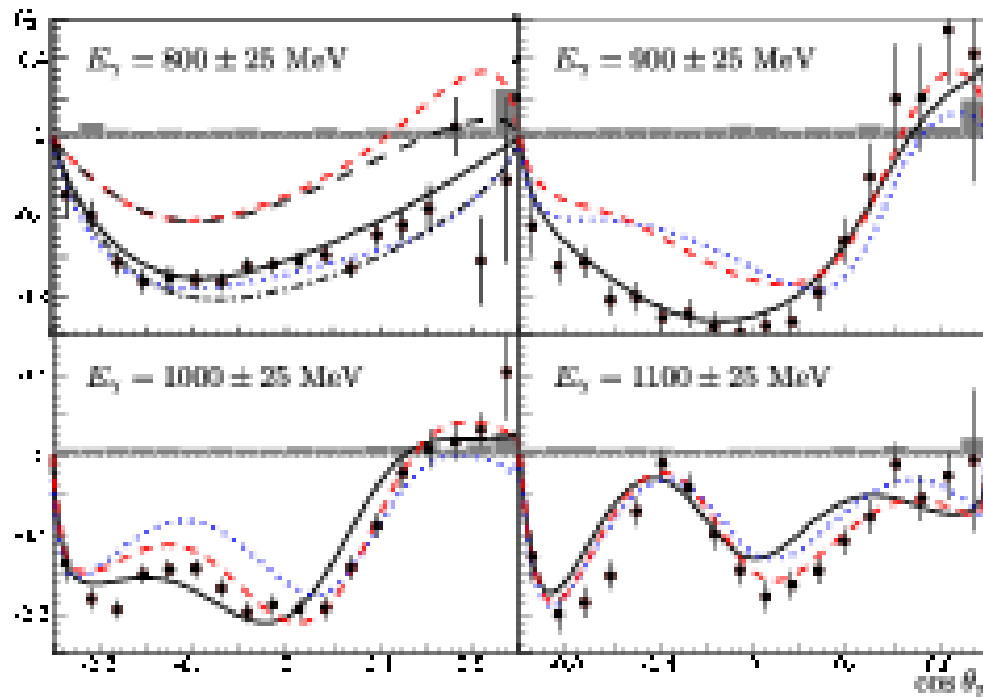


Figure 3. (Color online) The polarization observable G as a function of $\cos \theta_\gamma$ from $E_\gamma = 800$ MeV up to $E_\gamma = 1100$ MeV. Systematic errors are shown in gray bars. Curves: see fig. 2.

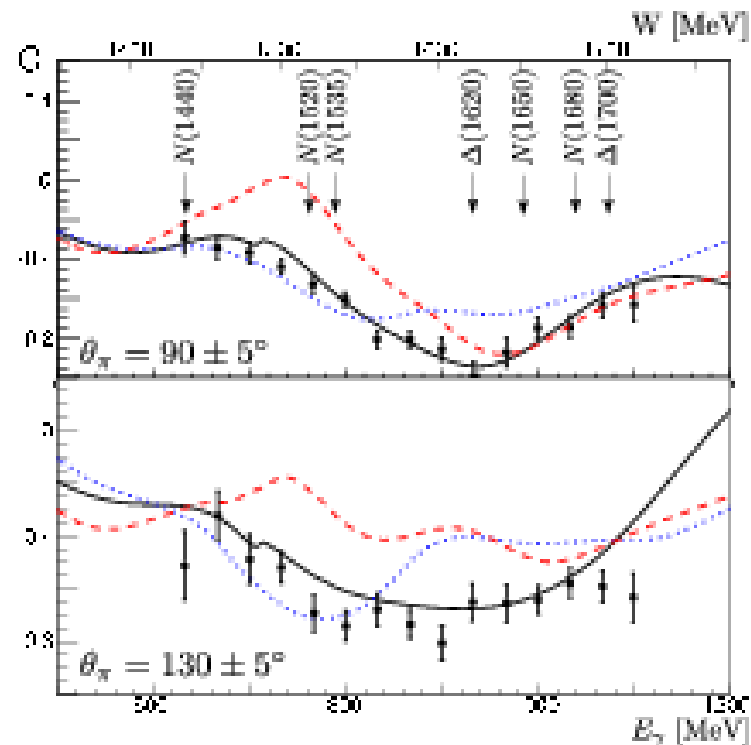


Figure 4. The double-polarization observable G as a function of energy for two selected bins in θ_π . Curves: see fig. 2. For comparison the positions of several resonances are marked.

Summarizing, we have reported the first measurement of the double-polarization observable G in the reaction $\vec{\gamma}\vec{p} \rightarrow p\pi^0$ in a wide range of energies and covering the full solid angle. The new data on G resolve the discrepant results on the helicity amplitudes of low-lying four-star nucleon resonances obtained from BnGa, MAID, and SAID and are an important step towards a complete data base which will define unambiguously the nucleon excitation spectrum.

Transparency ratio in $\gamma A \rightarrow \eta' A'$ and the in-medium η' width

M. Nanova¹, V. Metag¹, A. Ramos², E. Oset³, I. Jaegle^{4,a}, K. Makonyi¹, K. Brinkmann⁵,
O. Bartholomy⁵, D. Bayadilov^{5,6}, Y.A. Beloglazov⁶, V. Crede^{5,b}, H. Dutz⁵, A. Ehmans⁵,
D. Elsner⁷, K. Essig⁵, R. Ewald⁷, I. Fabry⁵, M. Fuchs⁵, Ch. Funke⁵, R. Gregor¹,
A.B. Gridnev⁶, E. Gutz⁵, S. Höffgen⁵, P. Hoffmeister⁵, I. Horn⁵, J. Junkersfeld⁵,
H. Kalinowsky⁵, Frank Klein⁷, Friedrich Klein⁷, E. Klempt⁵, M. Konrad⁷, B. Kopf^{8,9},
B. Krusche⁴, J. Langheinrich^{7,9}, H. Löhner¹⁰, I.V. Lopatin⁶, J. Lotz⁵, S. Lugert¹,
D. Menze⁷, T. Mertens⁴, J.G. Messchendorp¹⁰, C. Morales⁷, R. Novotny¹, M. Ostrick^{7,c},
L.M. Pant^{1,d}, H. van Pee⁵, M. Pfeiffer¹, A. Roy^{1,e}, A. Radkov⁶, S. Schadmand^{1,f},
Ch. Schmidt⁵, H. Schmieden⁷, B. Schoch⁷, A. Süle⁷, V. V. Sumachev⁶,
T. Szczepanek⁵, U. Thoma⁵, D. Trnka¹, R. Varma^{1,g}, D. Walther⁵, Ch. Wendel⁵
(The CBELSA/TAPS Collaboration)

Transparency ratio in $\gamma A \rightarrow \eta' A'$ and the in-medium η' width

Abstract

The photoproduction of η' -mesons off different nuclei has been measured with the CBELSA/TAPS detector system for incident photon energies between 1500 - 2200 MeV. The transparency ratio has been deduced and compared to theoretical calculations describing the propagation of η' -mesons in nuclei. The comparison indicates a width of the η' -meson of the order of $\Gamma = 15 - 25$ MeV at $\rho = \rho_0$ for an average momentum $p_{\eta'} = 1050$ MeV/c, at which the η' -meson is produced in the nuclear rest frame. The inelastic $\eta'N$ cross section is estimated to be 3 - 10 mb. Parameterizing the photoproduction cross section of η' -mesons by $\sigma(A) = \sigma_0 A^\alpha$, a value of $\alpha = 0.84 \pm 0.03$ has been deduced.

Transparency ratio is the ratio of production cross sections per nucleon in different nuclei with respect to the elementary cross section on the nucleon.

The photoproduction cross section $A(\gamma, \eta')A'$ in nuclei is not proportional to A for different nuclei, and the deviation from A scaling can be related to the width of the produced particle in the nucleus.

Tagged photons with energies of 0.9 - 2.2 GeV, produced via bremsstrahlung at a rate of 8-10 MHz, impinged on a solid target. For the measurements, ^{12}C , ^{40}Ca , ^{93}Nb and ^{208}Pb targets were used with thicknesses of 20, 10, 1, and 0.6 mm, respectively, each corresponding roughly to about 8-10% of a radiation length. The data were collected during two running periods totaling 575 h. Events with η' candidates were selected with suitable multiplicity trigger conditions requiring at least two hits in TAPS or at least one hit in TAPS and two hits in the CB, derived from a fast cluster recognition encoder. A more detailed description of the detector setup and the running conditions can be found in [28, 29].

The η' -mesons were identified via the $\eta' \rightarrow \pi^0\pi^0\eta \rightarrow 6\gamma$ decay channel, which has a branching ratio of 8.1%. For the reconstruction of the η' -meson, only events with at least 6 or 7 neutral hits were selected. Because of the competing channel $\eta \rightarrow \pi^0\pi^0\pi^0 \rightarrow 6\gamma$ with the same final state, this reaction was also reconstructed and the corresponding events were rejected from the further analysis. In addition, only events with one combination of the 6 photons to two photon pairs with mass $110 \text{ MeV}/c^2 \leq m_{\gamma\gamma} \leq 160 \text{ MeV}/c^2$ close to the π^0 mass and one pair with mass $500 \text{ MeV}/c^2 \leq m_{\gamma\gamma} \leq 600 \text{ MeV}/c^2$ close to the η mass were analyzed further.

(GAMMA-NUCLEON)

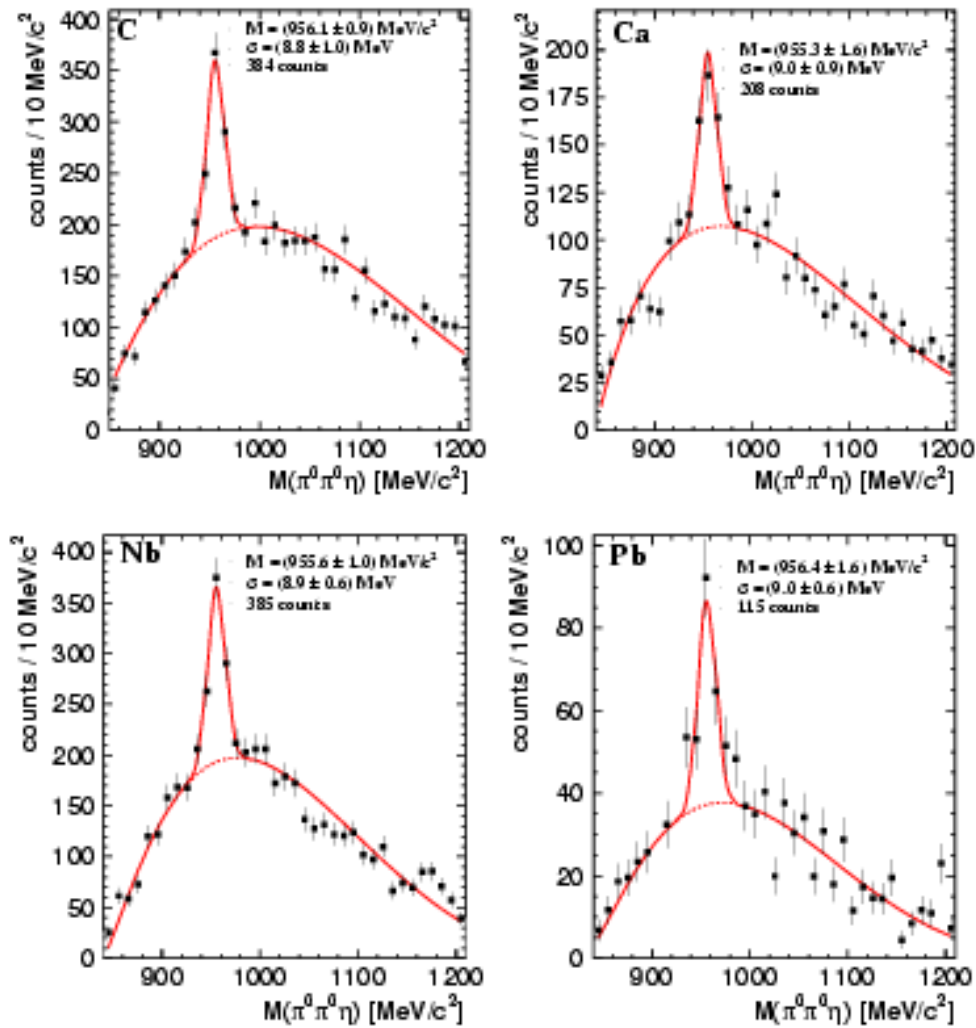


FIG. 1. Invariant mass spectrum of $\pi^0\pi^0\eta$ for ^{12}C , ^{40}Ca , ^{93}Nb and ^{208}Pb targets for the incident photon energy range 1500 - 2200 MeV. The solid curve is a fit to the spectrum. Only statistical errors are given. See text for more details.

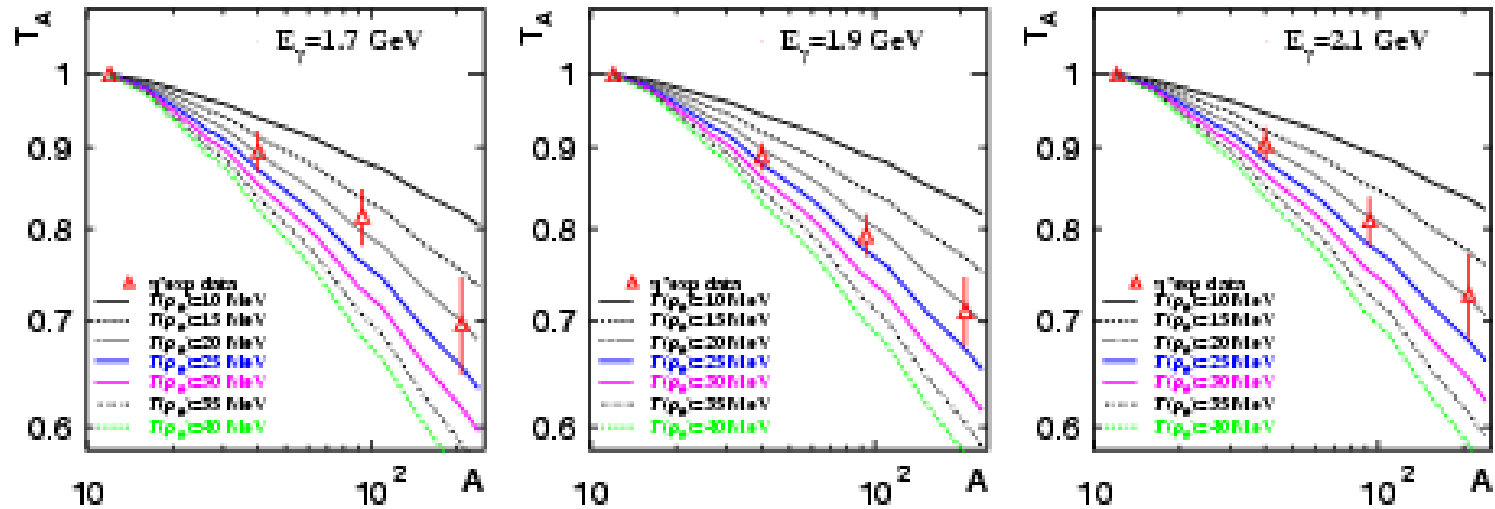


FIG. 2. Transparency ratio relative to that of ^{12}C , $T_A = \bar{T}_A/\bar{T}_{12}$, as a function of the nuclear mass number A , for different in-medium widths of the η' at three different incident photon energies. Only statistical errors are shown. The systematic errors are of the order of 20% but tend to partially cancel since cross section ratios are given.

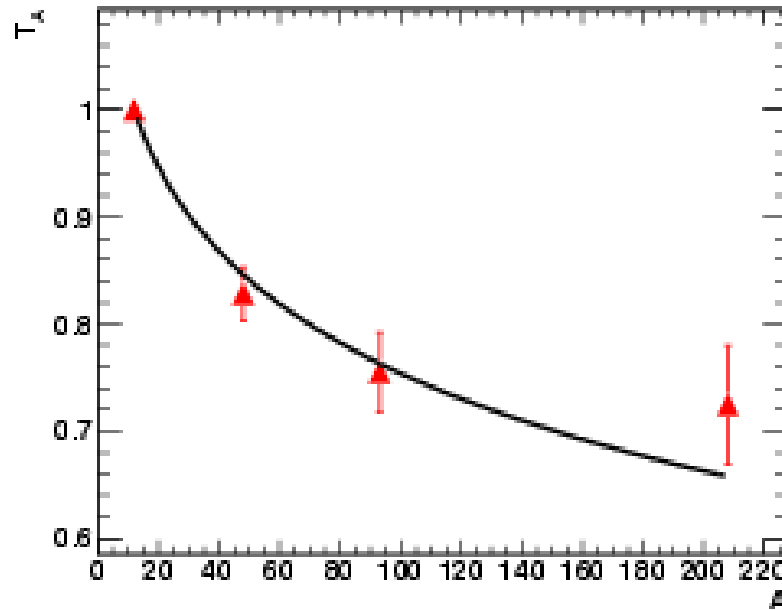


FIG. 3. The transparency ratio for η' -mesons as a function of the nuclear mass number A for the full incident photon energy range of 1500 - 2200 MeV. The solid curve is a fit to the data using expression in Eq.(11).

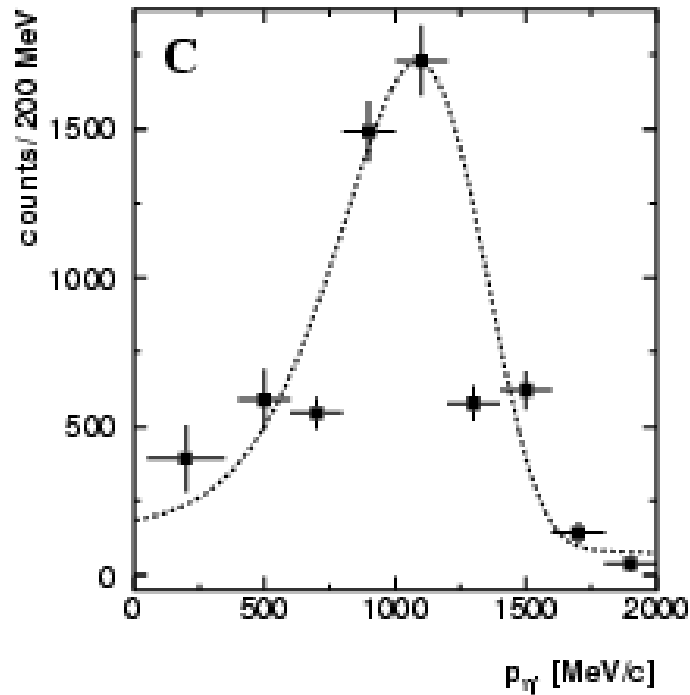


FIG. 4. Momentum distribution of η' -mesons produced off a C target for $E_\gamma^{beam} = 1500 - 2200$ MeV. The dashed curve is to guide the eye.

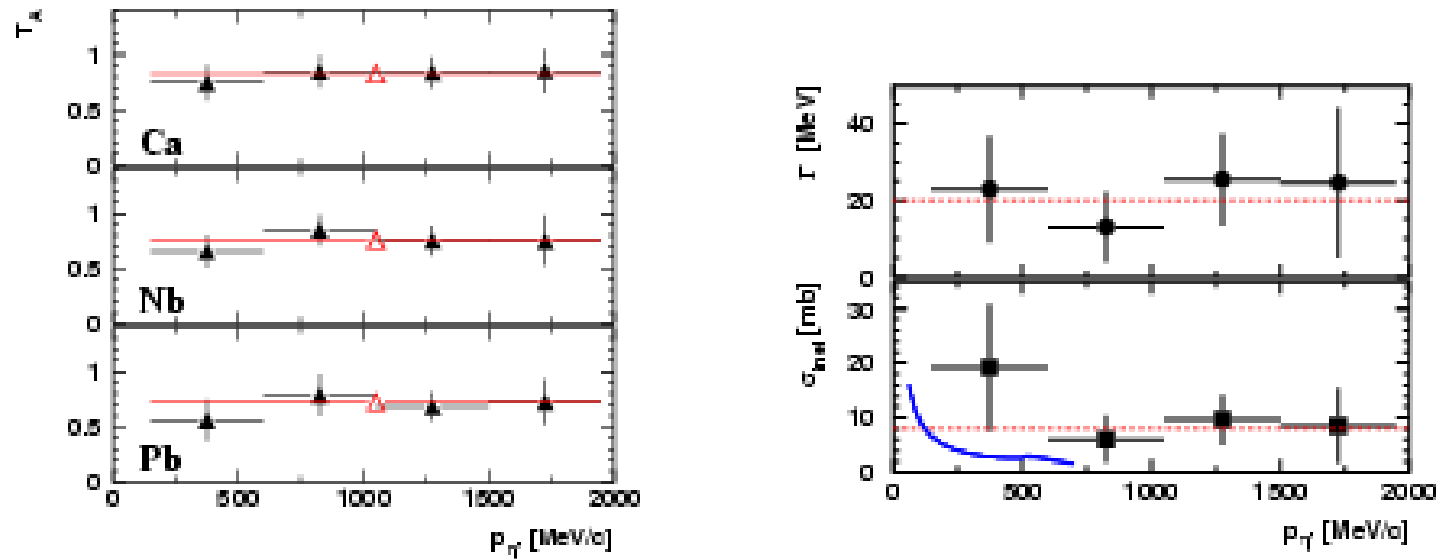


FIG. 5. (Left) Transparency ratio for the η' -meson normalized to C for three different targets: Ca, Nb, and Pb and four bins in η' momentum (full triangles) for the full incident photon energy range from 1500 - 2200 MeV. The open triangles show the values when integrated over all momenta and energies. (Right) The in-medium width (upper panel) and inelastic cross section (lower panel) as a function of the η' momentum. For comparison, the theoretical predictions for σ_{inel} [7] are shown by a blue (solid) curve.

III. CONCLUSIONS

The transparency ratios for η' -mesons measured for several nuclei deviate sufficiently from unity to allow an extraction of the η' width in the nuclear medium, and an approximate inelastic cross section for $\eta'N$ at energies around $\sqrt{s} \approx 2.0$ GeV. We find $\Gamma \approx 15 - 25$ MeV $\cdot \rho/\rho_0$ roughly, corresponding to an inelastic $\eta'N$ cross section of $\sigma_{\text{inel}} \approx 6-10$ mb. If inelastic and two-body absorption processes were equally strong the inelastic cross section would be reduced to $\sigma_{\text{inel}} \approx 3-5$ mb. Despite of the uncertainties and approximations involved in the determination of σ_{inel} , this is the first experimental measurement of this cross section. A comparison to photoproduction cross sections and transparency ratios measured for other mesons (π, η, ω) demonstrates the relatively weak interaction of the η' -meson with nuclear matter. Regarding the observability of η' mesic states the measured in-medium width of $\Gamma \approx 15 - 25$ MeV at normal nuclear matter density would require a depth of about 50 MeV or more for the real part of the η' - nucleus optical potential.

Гамма-мезон

Crystal Ball at MAMI, TAPS and A2 (Майнц)

Участники коллаборации
от Лаборатории мезонной физики:

В.С.Бекренёв, С.П.Круглов, А.А. Кулбардис

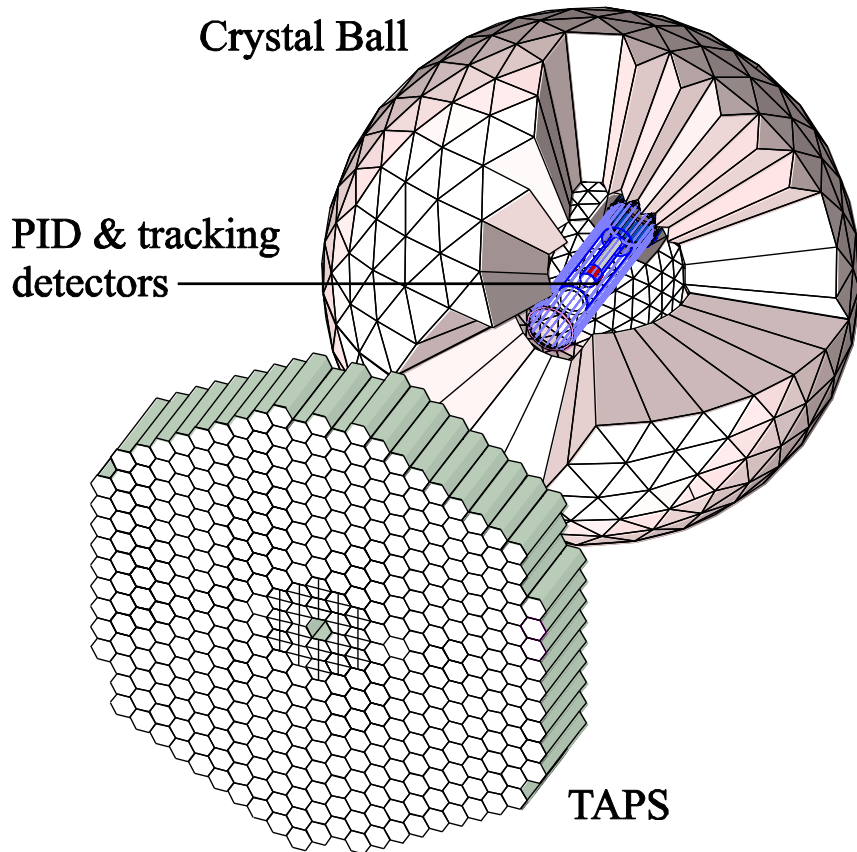
Crystal Ball:

- μ^\pm : 233 MeV
- π^\pm : 240 MeV
- K^\pm : 341 MeV
- p: 425 MeV

TAPS:

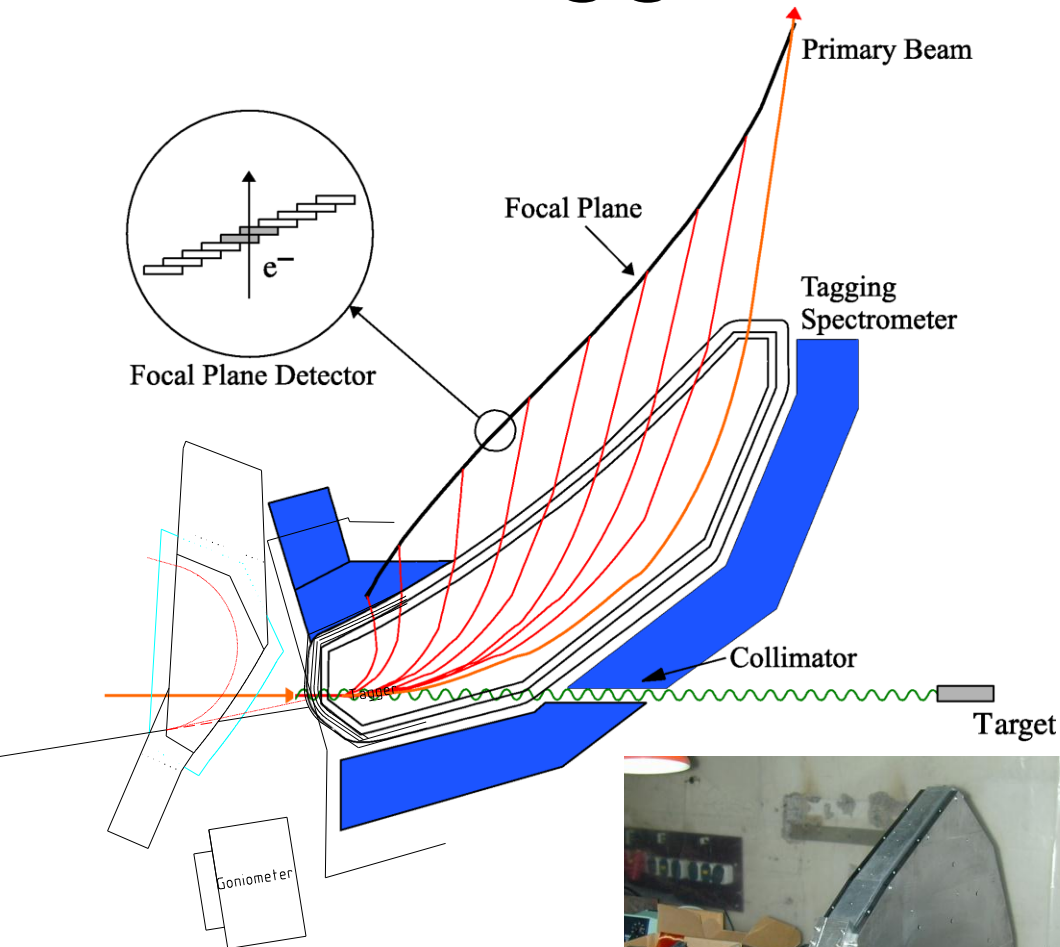
- μ^\pm : 165 MeV
- π^\pm : 180 MeV
- K^\pm : 280 MeV
- p: 360 MeV

Experimental Setup

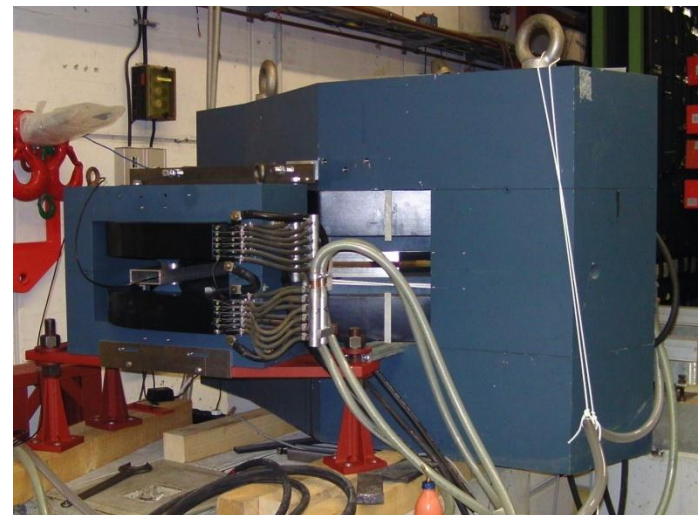


- **Crystal Ball:**
 - 672 NaI crystals about 16 *r.l.*
 - Cover 94% solid angle
 - Angular resolution: $\sigma(\varphi)$ is 2-3 degree and $\sigma(\Theta)$ is $(2^\circ-3^\circ)/\cos(\Theta)$
 - Energy resolution of about $\Delta E/E=0.02(E[\text{GeV}])^{0.36}$
- **TAPS:**
 - 366 BaF₂ and 72 PbWO crystals
 - Time resolution 160 psec
 - Overall acceptance for EC calorimeter 97%
- **PID:**
 - Barrel of 24, 4 mm thick plastic strips
 - Good time resolution
 - Proton identification using $\Delta E/\Delta x$
- **MWPC:**
 - Two-layers cylindrical chamber
 - Angular resolution 2-3 degrees
 - Minimum material in particular in forward direction

Tagged Photon Beam



- Maximum electron energy – 1604 MeV
- Maximum energy of tagged photons –
- 1453 MeV with the main tagger,
- and up to 1548 MeV with the end-point tagger
- Energy resolution ~ 4 MeV in the main tagged ladder, ~ 1 MeV resolution in the microscope



Study of the $\gamma p \rightarrow \pi^0 \pi^0 p$ reaction with the Crystal Ball/TAPS at the Mainz Microtron


L. Kashevarov^{1,2*}, A. Fix^{3†}, S. Prakhov⁴, P. Aguar-Bartolomé¹, J. R. M. Annand⁵, H. J. Arends¹, K. Bantaw
R. Beck⁷, V. Bekrenev⁸, H. Berghäuser⁹, A. Braghieri¹⁰, W. J. Briscoe¹¹, J. Brudvik⁴, S. Cherepnaya²,
R. F. B. Codling⁵, E. J. Downie^{1,5}, P. Drexler⁹, L. V. Fil'kov², D. I. Glazier¹², R. Gregor⁹, E. Heid^{1,11},
D. Hornidge¹³, L. Isaksson¹⁴, I. Jaegle¹⁵, O. Jahn¹, T. C. Jude¹², I. Keshelashvili¹⁵, R. Kondratiev¹⁶,
M. Korolija¹⁷, M. Kotulla⁹, A. Koulbardiš⁸, S. Kruglov⁸, B. Krusche¹⁵, V. Lisin¹⁶, K. Livingston⁵,
I. J. D. MacGregor⁵, Y. Maghrbi¹⁵, D. M. Manley⁶, J. C. McGeorge⁵, E. F. McNicoll⁵, D. Mekterovic¹⁷,
†. Metag⁹, A. Mushkarenkov¹⁰, B. M. K. Nefkens⁴, A. Nikolaev⁷, R. Novotny⁹, H. Ortega¹, M. Ostrick¹, P. Ott
‡. B. Otte¹, B. Oussena¹, P. Pedroni¹⁰, F. Pheron¹⁵, A. Polonski¹⁶, J. Robinson⁵, G. Rosner⁵, T. Rostomyan¹⁰,
S. Schumann^{1,7}, M. H. Sikora¹², D. I. Sober¹⁸, A. Starostin⁴, I. I. Strakovsky¹¹, I. M. Suarez⁴, I. Supek¹⁷,
C. M. Tarbert¹², M. Thiel⁹, A. Thomas¹, M. Unverzagt^{1,7}, D. P. Watts¹², D. Werthmüller¹⁵, and F. Zehr¹⁵

(Crystal Ball at MAMI, TAPS, and A2 Collaborations)

Study of the $\gamma p \rightarrow \pi^0 \pi^0 p$ reaction with the Crystal Ball/TAPS at the Mainz Microtron

The $\gamma p \rightarrow \pi^0 \pi^0 p$ reaction has been measured from threshold to 1.4 GeV using the Crystal Ball and TAPS photon spectrometers together with the photon tagging facility at the Mainz Microtron. The experimental results include total and differential cross sections as well as specific angular distributions, which were used to extract partial-wave amplitudes. In particular, the energy region below the $D_{13}(1520)$ resonance was studied.

(GAMMA-HYDROGEN)

The present measurement used 855-MeV and 1508-MeV electron beams from the upgraded Mainz Microtron, MAMI-C [31]. The data with the 1508-MeV beam were taken in 2007, and with the 855-MeV beam in 2008. Bremsstrahlung photons, produced by the 1508-MeV electrons in a 10- μm Cu radiator and collimated by a 4-mm-diameter Pb collimator, were incident on a 5-cm-long liquid hydrogen (1H_2) target located in the center of the CB. The energies of the incident photons were measured in the range 617 to 1402 MeV by detecting the post-bremsstrahlung electrons in the Glasgow tagger [32]. With the 855-MeV electron beam, bremsstrahlung photons were produced in a diamond radiator, collimated by a 3-mm-diameter Pb collimator, and incident on a 10-cm-long 1H_2 target. In this experiment, the energies of the incident photons were tagged from 84 to 796 MeV. The energy resolution of the tagged photons is mostly defined by the width of the tagger focal plane detectors, and by the electron beam energy. For a beam energy of 1508 MeV, a typical width of a tagger channel was about 4 MeV, and about 2 MeV for a beam energy of 855 MeV. Due to the beam collimation only part of the bremsstrahlung photon flux reached the 1H_2 target. 

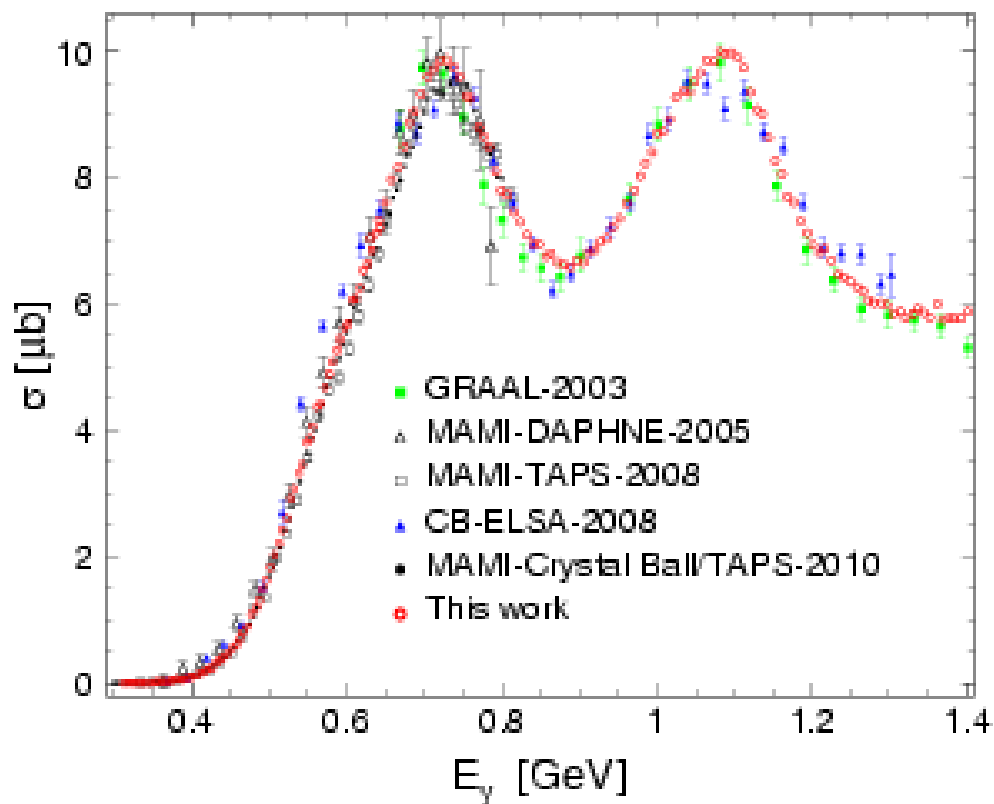


FIG. 1: (Color online) Total cross sections for $\gamma p \rightarrow \pi^0 \pi^0 p$ are shown as a function of the incident-photon energy. The results obtained in this work are compared to the existing data from GRAAL [6], CB-ELSA [11, 12], DAPHNE [8], TAPS [12], and Crystal Ball/TAPS [40]. Only statistical uncertainties are shown for all data.

(GAMMA-NUCLEON)

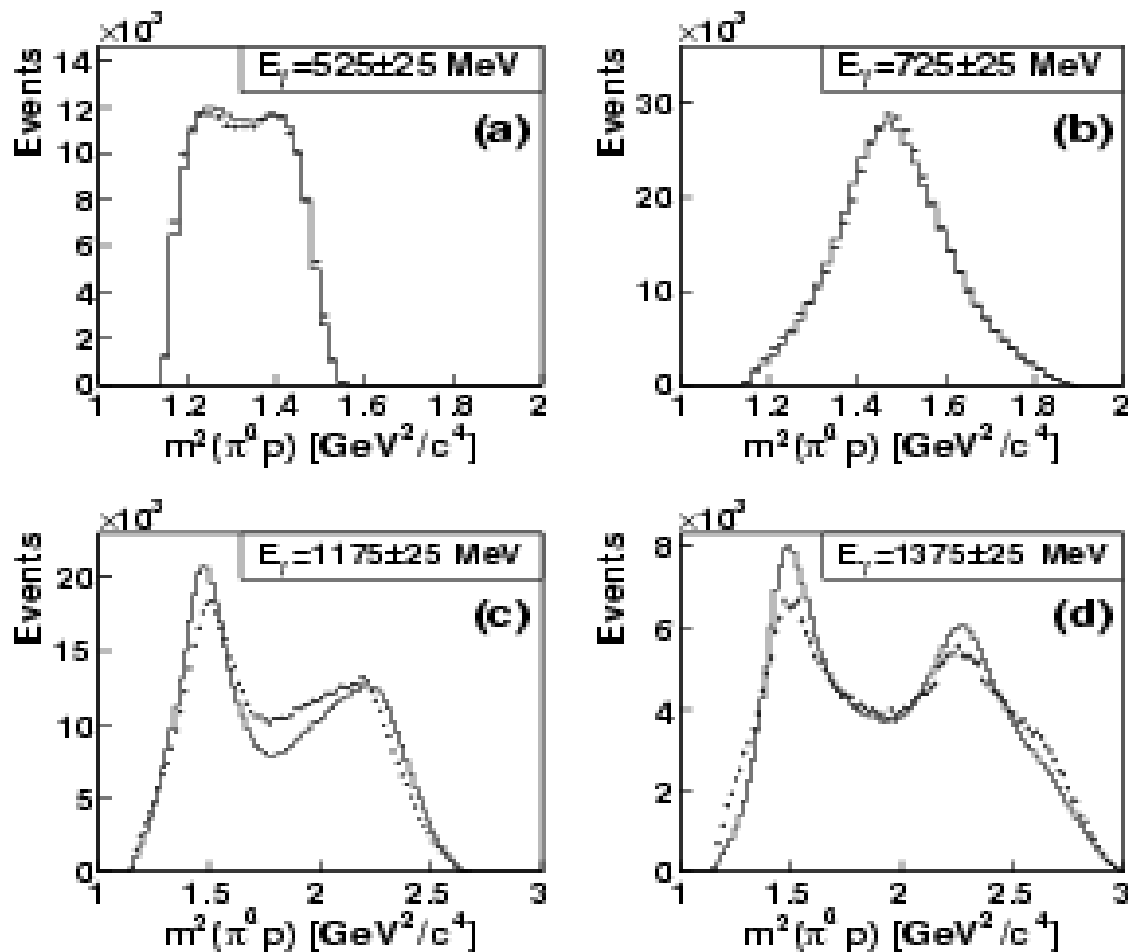


FIG. 2: Experimental $m^2(\pi^0 p)$ invariant-mass distributions (crosses) compared to those obtained from the MC simulation (solid line) of the $\gamma p \rightarrow \pi^0 \pi^0 p$ reaction. The MC event generation included the $\Delta\pi^0$ and $D_{13}(1520)\pi^0$ intermediate states in double- π^0 photoproduction.

ГАММА-ИЗЛУЧЕНИЕ

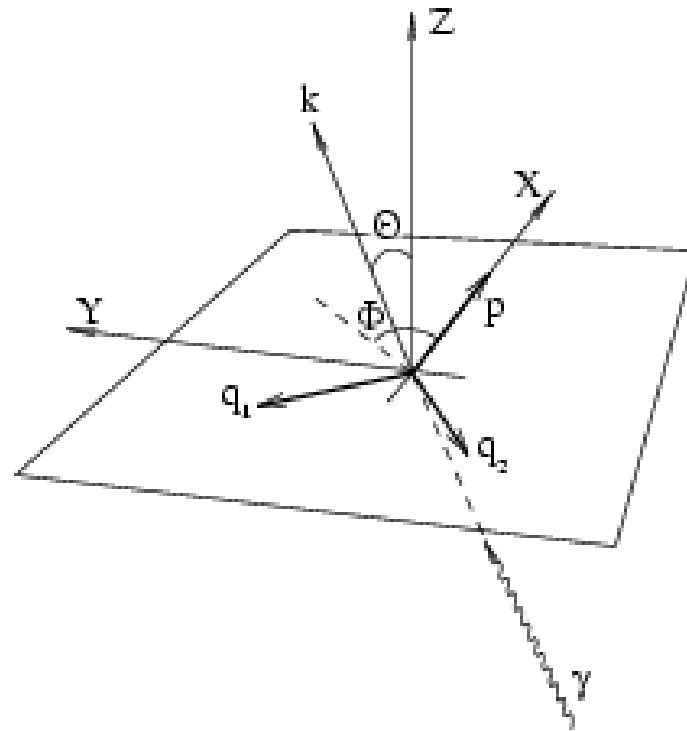


FIG. 3: Definition of the coordinate system used in the present formalism. \vec{k} , \vec{p} , \vec{q}_1 , and \vec{q}_2 are respectively three-momenta of the incident-photon, out-going proton, two pions in the center of mass system. Axis Z is a normal to the decay plane. Axis X is along \vec{p} . Θ and Φ are respectively the polar and azimuthal angles of \vec{k} .

$$\begin{aligned}
 W(\Theta, \Phi) &\equiv \frac{1}{\sigma} \frac{d\sigma}{d\Omega} \\
 &= \sum_{L \geq 0} \sum_{M=-L}^L \sqrt{\frac{2J+1}{4\pi}} W_{LM} Y_{LM}(\Theta, \Phi), \quad (3)
 \end{aligned}$$

which is expanded over spherical harmonics with $W_{00} = 1$. The coefficients W_{LM} in Eq. (3) are hermitian combinations of the partial-wave amplitudes $t_{\nu\mu}^{JM}$. The corresponding expression was obtained in [26]:

$$\begin{aligned}
 W_{LM} &= \frac{\pi}{\sigma} \mathcal{K} \int d\omega_1 d\omega_2 \sum_{\nu\mu} \sum_{JJ' M_j M'_j} (-1)^{M+\mu} \\
 &\times C_{J'M'_j, JM_j}^{LM} C_{J'\mu J-\mu}^{L0} t_{\nu\mu}^{J'M'_j}(\omega_1, \omega_2)^* t_{\nu\mu}^{JM_j}(\omega_1, \omega_2), \quad (4)
 \end{aligned}$$

where \mathcal{K} is an appropriate phase space factor. Formula (3) determines the general structure of an angular distribution in a manner analogous to the expansion of the cross section for single-meson photoproduction in terms of the Legendre polynomials.

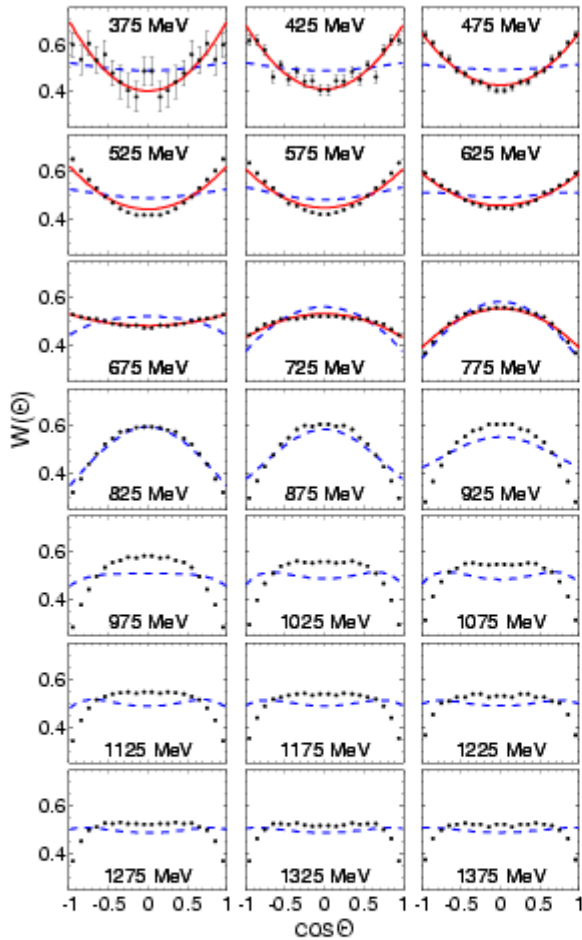


FIG. 4: (Color online) Distribution $W(\Theta) = \int W(\Theta, \Phi) d\Phi$ shown as a function of $\cos \Theta$, where Θ is the polar angle of the incident photon in the coordinate frame presented in Fig. 3. Our experimental results with statistical uncertainties are shown by filled circles. The predictions from the model of Ref. [19] are shown by dashed lines. The results of fitting our data below $E_\gamma = 0.8$ GeV are shown by solid lines. The energy label in each panel indicates the central photon energy for each bin.

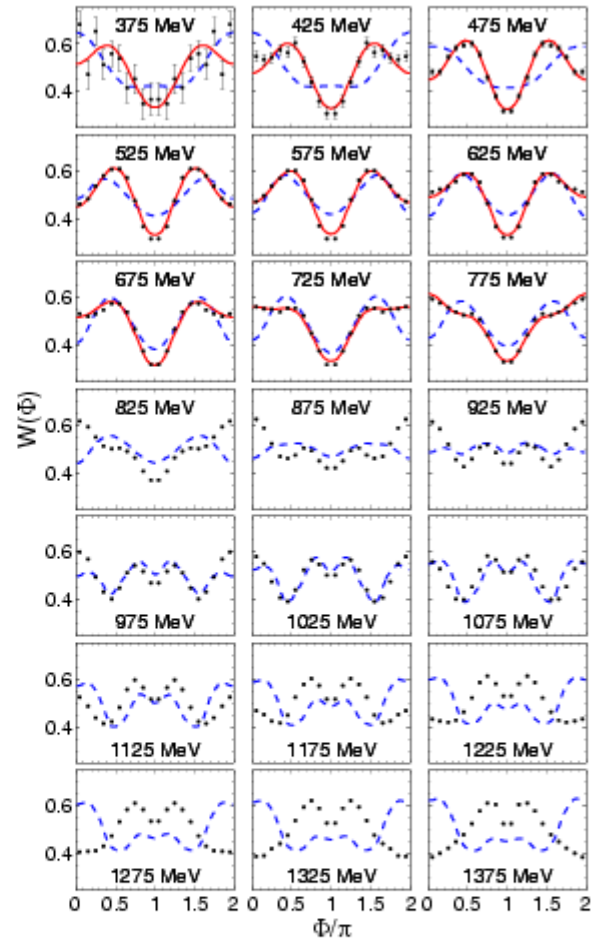


FIG. 5: (Color online) Distribution $W(\Phi) = \pi \int W(\Theta, \Phi) \sin \Theta d\Theta$, where Φ is the azimuthal angle of the incident photon in the coordinate frame presented in Fig. 3. Other notations are the same as in Fig. 4.

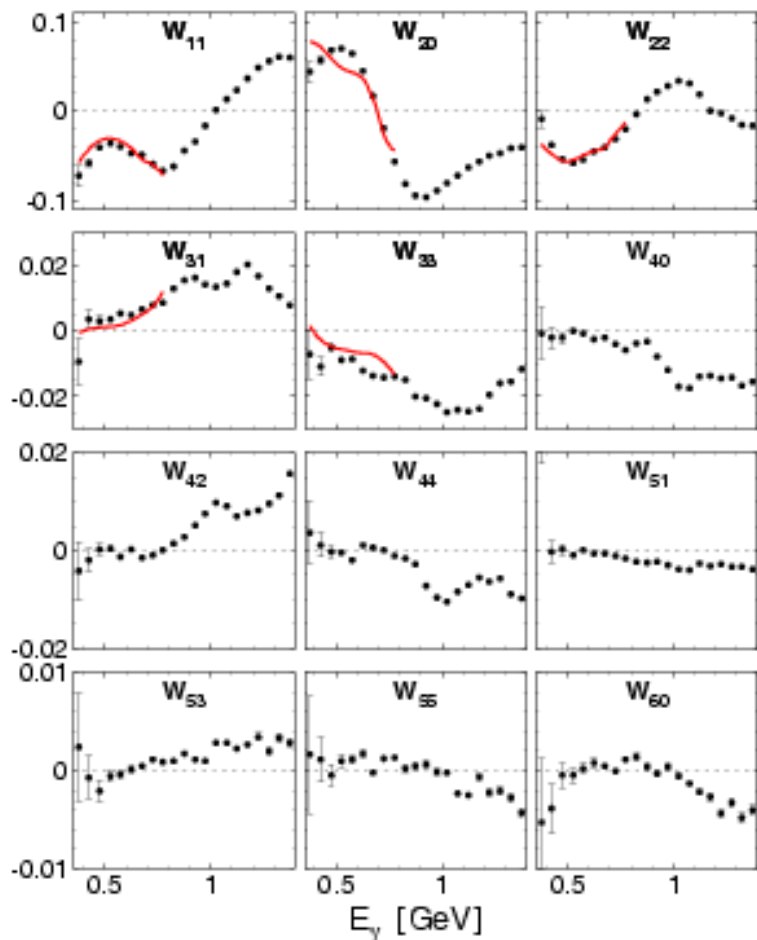


FIG. 6: (Color online) Moments W_{LM} (normalized such that $W_{00} = 1$) as a function of the incident-photon energy. Our experimental results for the real part of W_{LM} are shown by filled circles. The fit results are shown by solid lines.

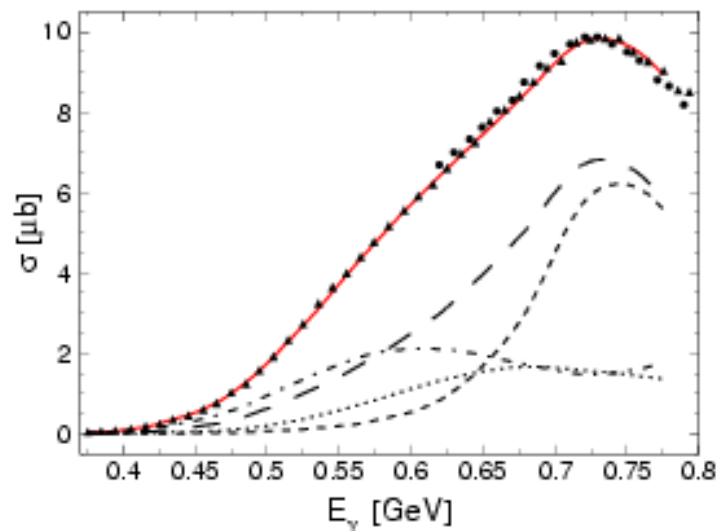


FIG. 7: (Color online) Total cross section for $\gamma p \rightarrow \pi^0 \pi^0 p$ as a function of the incident-photon energy. Our experimental results are shown by triangles and circles, respectively for the data with the 855-MeV and 1508-MeV electron beam. Only statistical uncertainties are shown. The fit results for the total cross section are shown by the solid line, and for the $3/2^-$, $3/2^+$, and $1/2^+$ waves by long-dashed, dash-dotted, and dotted lines, respectively. The $D_{13}(1520)$ contribution, calculated from the model of Ref. [19], is shown by the short-dashed line.

(GAMMA-NUCLEON)

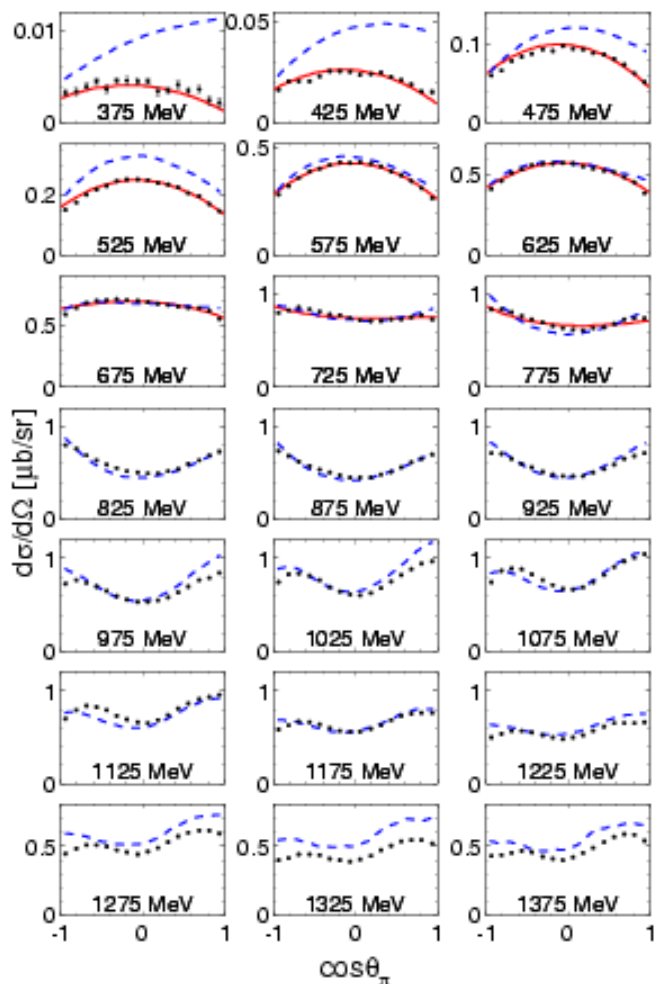


FIG. 8: (Color online) $\gamma p \rightarrow \pi^0 \pi^0 p$ differential cross sections as a function of the production angle of the outgoing π^0 in the center of mass frame. Since there are two identical pions, each cross section represents the average of two distributions. Our experimental results with statistical uncertainties are shown by filled circles. The predictions from our model are shown by solid lines. The dashed lines result from the Bonn-Gatchina model [11, 12].

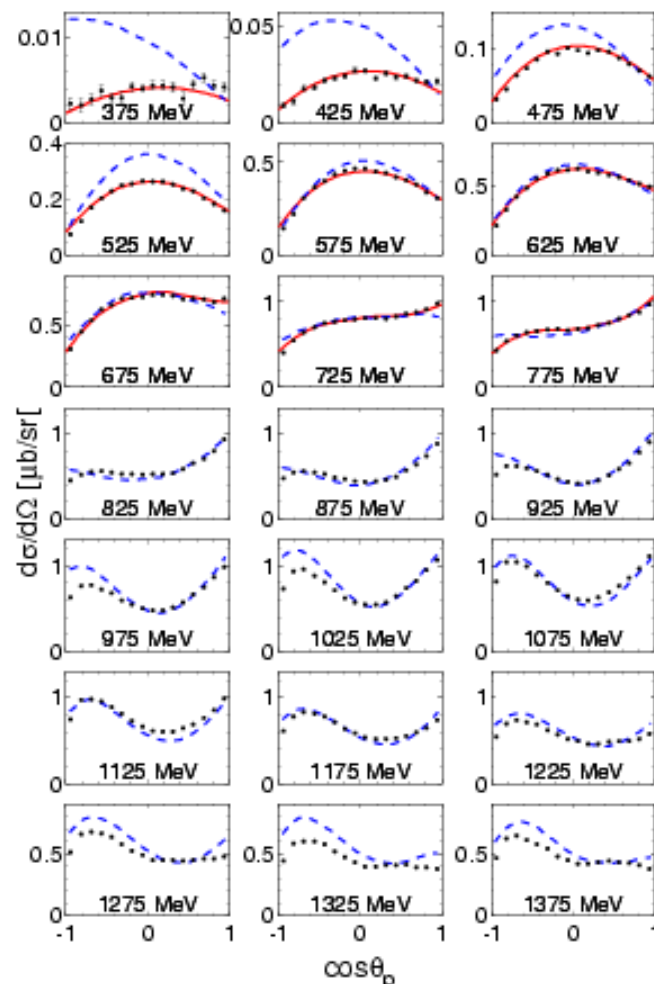


FIG. 9: (Color online) Same as Fig. 8 but for the outgoing proton.

ГAMMA-НУКЛИОН

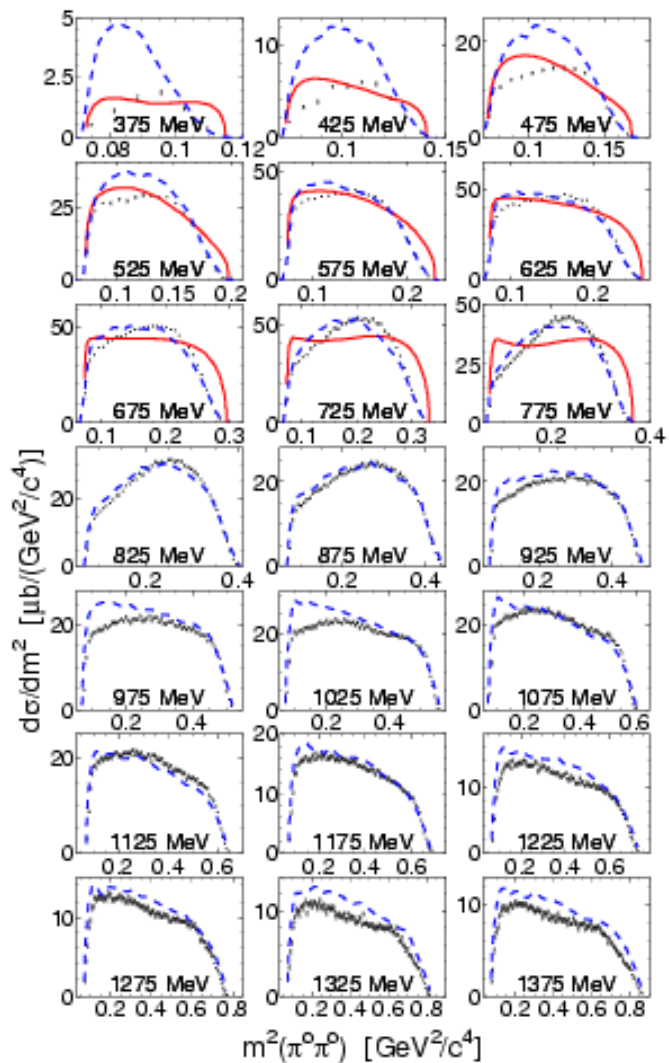


FIG. 10: (Color online) $\gamma p \rightarrow \pi^0 \pi^0 p$ differential cross sections as a function the invariant mass squared $m^2(\pi^0 \pi^0)$. Our experimental results with statistical uncertainties are shown by filled circles. The predictions from our model are shown by solid lines. The dashed lines result from the Bonn-Gatchina model [11, 12].

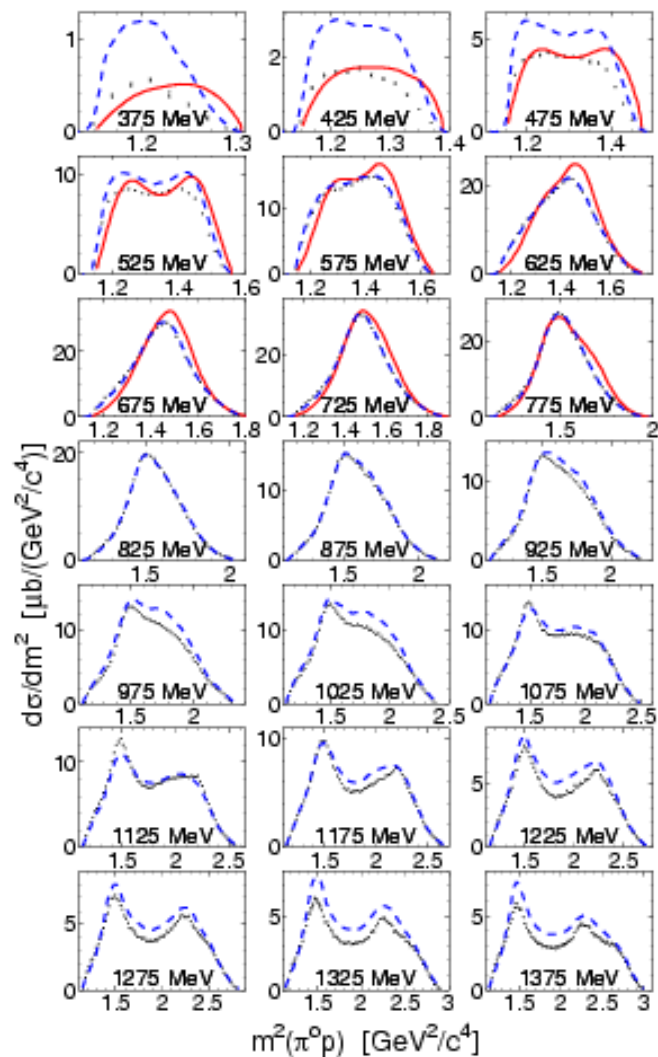


FIG. 11: (Color online) Same as Fig. 10, but for $m^2(\pi^0 p)$. Since there are two identical pions, each cross section represents the average of two distributions.

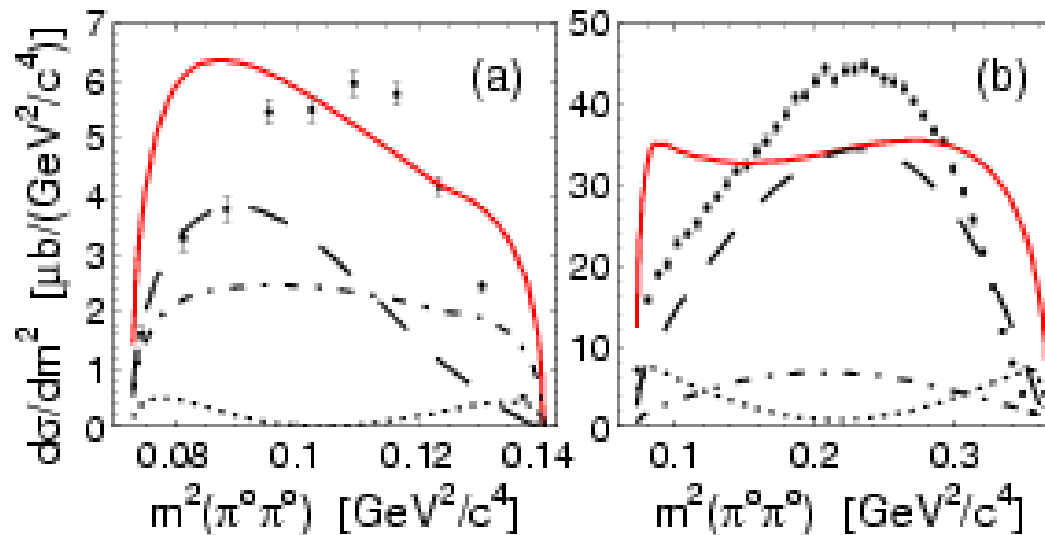


FIG. 12: (Color online) The partial wave contributions to the $\pi\pi$ spectrum for $E_\gamma = 425$ (a) and 775 MeV (b) (enlarged from Fig. 10). Long-dashed, dash-dotted, and dotted lines correspond to the $3/2^-$, $3/2^+$, and $1/2^+$ waves, respectively. The sum of all waves is shown by solid lines.

Our analysis of the energy dependence of W_{LM} showed that a large contribution from the $J = 3/2$ waves is necessary not only in the region of $D_{13}(1520)$ but also at energies below. According to our results, these waves seem to be responsible for an almost linear rise of the $\gamma p \rightarrow \pi^0 \pi^0 p$ total cross section in the region $E_\gamma = 450 - 725$ MeV. Isobar models with the dominant contribution from $D_{13}(1520)$ and a moderate role for the Roper resonance cannot explain such features in double- π^0 photoproduction. Whether these features are the reflection of a large $J^\pi = 3/2^+$ fraction of $\pi^+ \pi^- \rightarrow \pi^0 \pi^0$ rescattering, or are a consequence of the strong $D_{33}(1700)$ excitation, found in Ref. [12], requires further experimental and theoretical studies.

Coherent photoproduction of η -mesons off ^3He - search for η -mesic nuclei

F. Pheron ^a, J. Ahrens ^b, J.R.M. Annand ^c, H.J. Arends ^b, K. Bantawa ^d, P.A. Bartolome ^b, R. Beck ^e, V. Bekrenev ^f, H. Berghäuser ^g, B. Boillat ^a, A. Braghieri ^h, D. Branford ⁱ, W.J. Briscoe ^j, J. Brudvik ^k, S. Cherepnaya ^l, B. Demissie ^j, M. Dieterle ^a, E.J. Downie ^{b,c,j}, P. Drexler ^g, D.I. Glazier ⁱ, E. Heid ^b, L.V. Fil'kov ^l, D. Hornidge ^m, D. Howdle ^c, O. Jahn ^b, I. Jaegle ^a, T.C. Jude ⁱ, V.L. Kashevarov ^{l,b}, I. Keshelashvili ^a, R. Kondratiev ⁿ, M. Korolija ^o, M. Kotulla ^{a,g}, A. Kulbardis ^f, S.P. Kruglov ^f, B. Krusche ^a, V. Lisin ⁿ, K. Livingston ^c, I.J.D. MacGregor ^c, Y. Maghrbi ^a, J. Mancell ^c, D.M. Manley ^d, Z. Marinides ^j, M. Martinez ^b, J.C. McGeorge ^c, E. McNicoll ^c, D. Mekterovic ^o, V. Metag ^g, S. Micanovic ^o, D.G. Middleton ^m, A. Mushkarenkov ^h, B.M.K. Nefkens ^k, A. Nikolaev ^e, R. Novotny ^g, M. Oberle ^a, M. Ostrick ^b, B. Oussena ^{b,j}, P. Pedroni ^h, A. Polonski ⁿ, S.N. Prakhov ^k, J. Robinson ^c, G. Rosner ^c, T. Rostomyan ^{a,h}, S. Schumann ^b, M.H. Sikora ⁱ, D.I. Sober ^p, A. Starostin ^k, I. Supek ^o, M. Thiel ^g, A. Thomas ^b, M. Unverzagt ^b, D.P. Watts ⁱ, D. Werthmüller ^a, L. Witthauer ^a, F. Zehr ^a

Coherent photoproduction of η -mesons off ^3He - search for η -mesic nuclei

Abstract

Coherent photoproduction of η -mesons off ^3He , i.e. the reaction $\gamma^3\text{He} \rightarrow \eta^3\text{He}$, has been investigated in the near-threshold region. The experiment was performed at the Glasgow tagged photon facility of the Mainz MAMI accelerator with the combined Crystal Ball - TAPS detector. Angular distributions and the total cross section were measured using the $\eta \rightarrow \gamma\gamma$ and $\eta \rightarrow 3\pi^0 \rightarrow 6\gamma$ decay channels. The observed extremely sharp rise of the cross section at threshold and the behavior of the angular distributions are evidence for a strong $\eta^3\text{He}$ final state interaction, pointing to the existence of a resonant state. The search for further evidence of this state in the excitation function of π^0 -proton back-to-back emission in the $\gamma^3\text{He} \rightarrow \pi^0 p X$ reaction revealed a very complicated structure of the background and could not support previous conclusions.

2. Experiment and analysis

The experiment was performed at the tagged photon beam of the Mainz MAMI accelerator [50,51]. The electron beam of 1508 MeV was used to produce bremsstrahlung photons in a copper radiator of $10\mu\text{m}$ thickness, which were tagged with the upgraded Glasgow magnetic spectrometer [52–54] for photon energies from 0.45 GeV to 1.4 GeV. The typical bin width for the photon beam energy (4 MeV) is defined by the geometrical size of the plastic scintillators in the focal plane detector of the tagger. The intrinsic resolution of the magnetic spectrometer is better by more than an order of magnitude. The size of the tagged photon beam spot on the target was restricted by a 3 mm diameter collimator placed downstream from the radiator foil. The target was a mylar cylinder of 3.0 cm diameter and 5.08 cm length filled with liquid ^3He at a temperature of 2.6 K. The corresponding target density was 0.073 nuclei/barn.

The reaction products were detected with an electromagnetic calorimeter combining the Crystal Ball detector (CB) [55] made of 672 NaI crystals with 384 BaF₂ crystals from the TAPS detector [56,57], configured as a forward wall. The Crystal Ball was equipped with an additional Particle Identification Detector (PID) [58] for the identification of charged particles {

Гамма-излучение

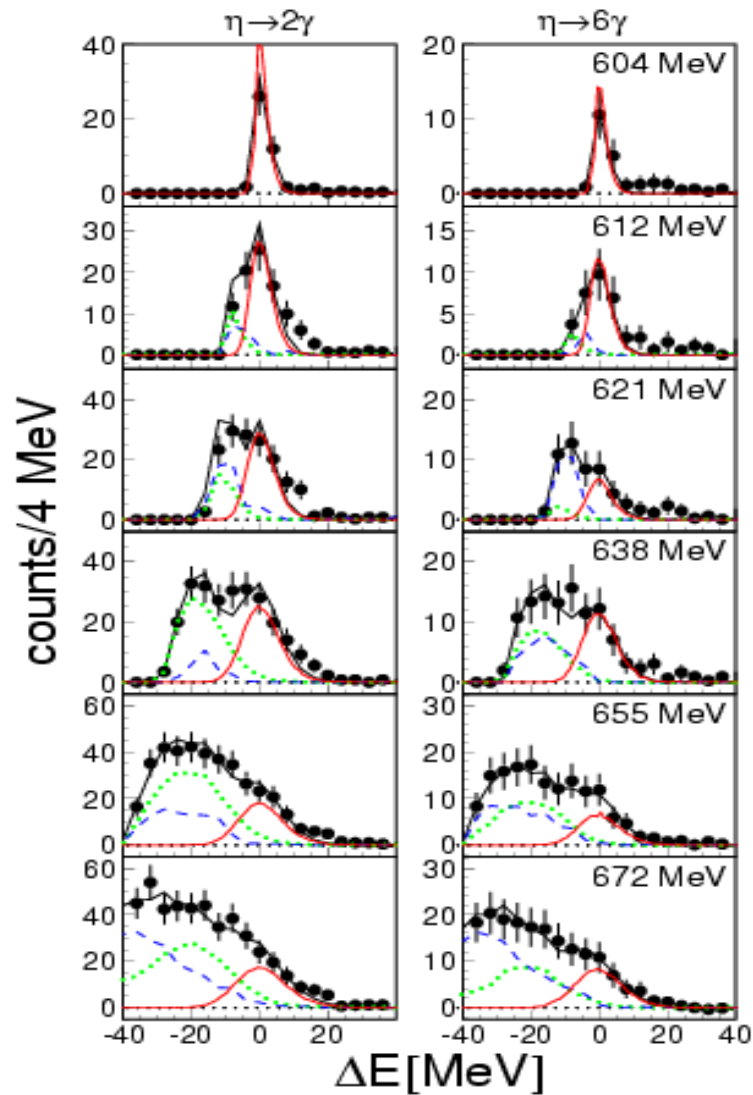


Fig. 1. Missing energy spectra for the $\gamma^3\text{He} \rightarrow \eta^3\text{He}$ reaction for the two-photon and $3\pi^0$ decay modes for different ranges of incident photon energy. Black dots: experiment. Curves: Monte Carlo simulations. Solid (red): coherent contribution, dashed (blue): recoil taken by quasi-free nucleon, dotted (green): recoil taken by di-nucleon, solid (black) sum of all.

(ГAMMA-ИЗЛУЧЕНИЕ)

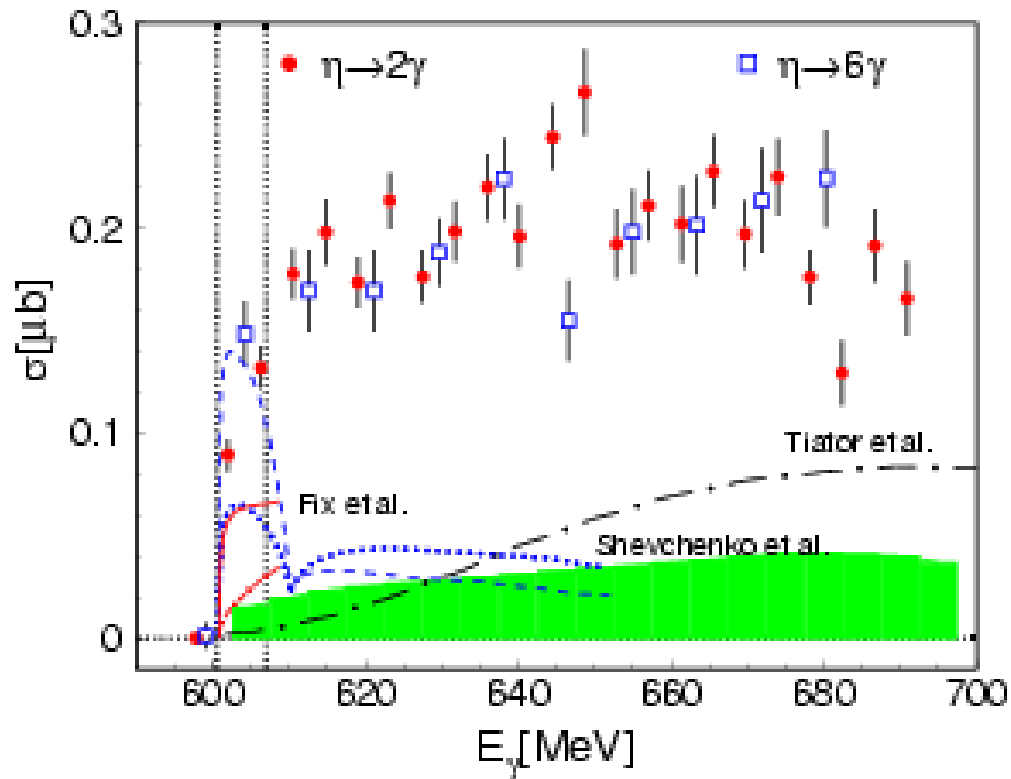


Fig. 2. Total cross section for the $\gamma^8\text{He} \rightarrow \eta^8\text{He}$ reaction from $\eta \rightarrow 2\gamma$ and $\eta \rightarrow 6\gamma$ decays. The shaded band at the bottom indicates the systematic uncertainty. The two vertical lines indicate coherent and breakup threshold. Theory curves: (blue) dotted and dashed from Shevchenko et al. [66] for two different versions of elastic ηN scattering, (red) solid (dash-dotted): Fix and Arenhövel [65] full model (plane wave), (black) long dash-dotted: Tiator et al. [64].

ГЛАВНОЕ (ГΑΜΜΑ-ΗΥΠΕΡΟΝ)

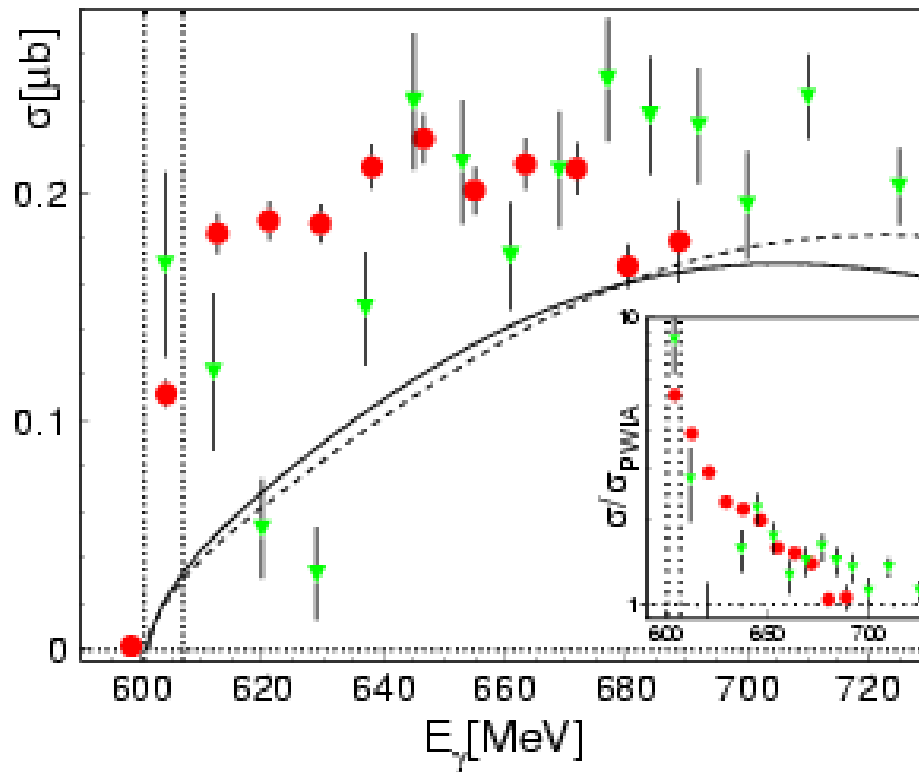


Fig. 3. Total cross section for $\gamma^3\text{He} \rightarrow \eta^3\text{He}$ (averaged over 2γ and $3\pi^0$ decays) (red dots) compared to previous data [47] (green triangles). Solid (dashed) curves: PWIA with realistic (isotropic) angular distribution for $\gamma n \rightarrow n\eta$ (see text). The present data are binned in the same way as the angular distributions in Fig. 4 (bin width ≈ 8 MeV). Insert: ratio of measured and PWIA cross sections.

(GAMMA-NUCLEON)

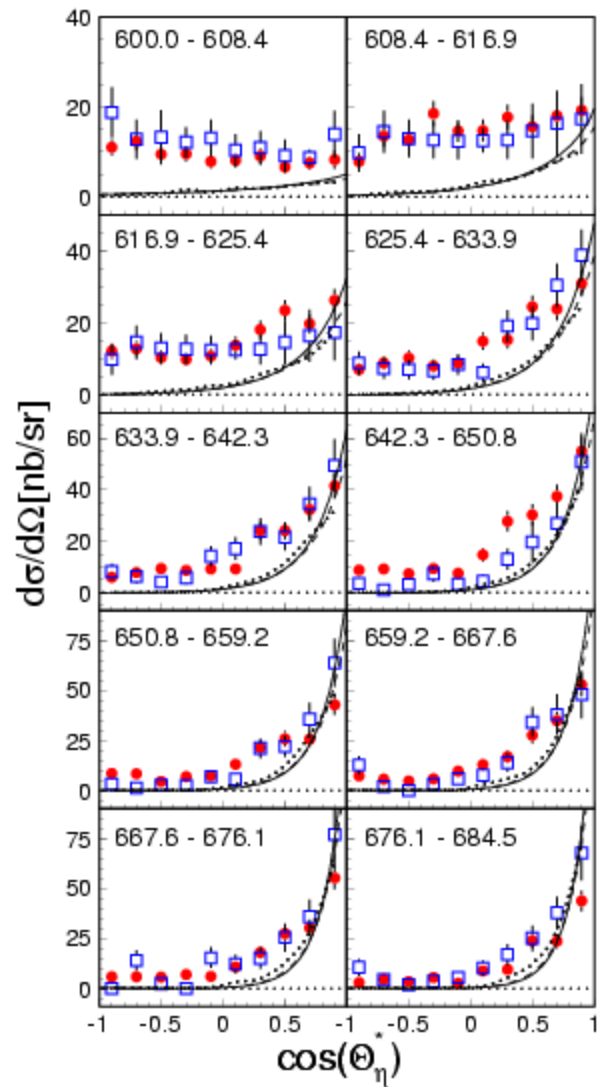


Fig. 4. Angular distributions of $\gamma^3\text{He} \rightarrow \eta^3\text{He}$ in the photon-nucleon c.m. system for different energy bins (range of incident photon energy in MeV indicated by the labels). (Red dots: $\eta \rightarrow 2\gamma$ decay, (blue) open squares: $\eta \rightarrow 6\gamma$ decay, dashed curves: results of PWIA model with isotropic angular distributions for $\gamma n \rightarrow n\eta$, solid curves with realistic angular distributions, dotted curves: folded with experimental resolution. (see text).

4. Summary and conclusions

Coherent photoproduction of η -mesons off ${}^3\text{He}$ has been measured with much improved statistical quality compared to the pilot experiment of Pfeiffer et al. [47]. The total cross section rises sharply between the coherent and breakup thresholds. Compared to a PWIA, which is in fair agreement with the data in the S_{11} peak, the threshold values are enhanced by nearly one order of magnitude. This is very different e.g. from the behavior of coherent η photoproduction off the deuteron, which is in reasonable agreement with PWIA [15]. The angular distributions at threshold are almost isotropic, and are unlike the forward peaked distributions expected to result from the form factor behavior. This result is similar to that previously observed for the hadron induced reactions $pd \rightarrow \eta^3\text{He}$ [37] and $dp \rightarrow \eta^3\text{He}$ [38–40]. This independence from the initial state is strong evidence for dominant η -nucleus interaction effects, related to a resonant state in the vicinity of the η production threshold.